Abnormal Growth of Electrodeposited BiSb Alloy Nanotubes

Xincun Dou, Guanghai Li,* Xiaohu Huang, and Liang Li

Key Laboratory of Materials Physics, Anhui Key Laboratory of Nanomaterials and Nanotechnology Institute of Solid State Physics, Chinese Academy of Sciences, Hefei 230031, People's Republic of China

Received: January 17, 2008; Revised Manuscript Received: March 10, 2008

BiSb alloy nanotube−nanowire array has been fabricated by the pulsed electrodeposition technique. It was found that the growth of the polycrystalline nanotubes is terminated by polycrystalline nanowires abruptly and then follows by single crystalline nanowires. The formation mechanism of the nanotubes and the origin of the transition from a polycrystalline nanotube to a polycrystalline nanowire were analyzed and discussed from the perspective of the crystal growth theory. The deep understanding of the transition is of high importance for the controlled synthesis and application in thermoelectric field of Bi-based nanotubes arrays.

Introduction

One-dimensional (1D) nanostructures have stimulated extensive research efforts in recent years because of their unique electrical, optical, and magnetic properties different from that of bulk and nanoparticles as well as their potential applications in mesoscopic research and nanodevices.[1–3] Different methods have been developed for the fabrication 1D nanostructures, Among these methods, the electrochemical deposition technique incorporated with the template method has proven to be a versatile approach for the preparation of ordered 1D metal arrays, such as nanowires, nanotubes, and junction structures of various materials with either single crystalline or polycrystalline structure, because it provides many outstanding advantages that are superior to other approaches.[4,5] Generally, the anodic alumina membrane (AAM) with fully covered gold electrode is used to grow nanowires as that with partially covered one favors the growth of nanotubes.[6–17]

Many works have contributed to the growth mechanism of the electrodeposited nanowires,[18–20] and it is generally considered that the growth mechanism of the electrodeposited single crystalline nanowires follows a 3D to 2D transition mode. As for the 2D growth mode, it is commonly recognized as a plane growth mode. For the growth of electrodeposited nanotubes, different mechanisms have also been proposed. Davis et al. [21–23] pointed out that both the gas evolution, resulted from the electrodeposition, and the partial pore coverage on the bottom of the membranes are accounted for the tube formation. Fukunaka et al.[8,24] proposed that the metal deposition rate must be balanced with the hydrogen generation rate in the formation of nanotubes and pointed out that the suppression of hydrogen bubble evolution in the nanocapillary structure plays an important role and metallic nanotubes cannot be fabricated by the electrodeposition if the growing grains readily become comparable to an employed pore size. Yoo et al.[25] considered that the deposition of a metal nanotube is a result of a nonuniform electric field concentrated at the edge tip of the initial tube structure created from a prior Au sputtering step, but the bottom side should be nanowires if under a relative low-current-density condition. Nevertheless, the study on the initial formation of the electrodeposited nanotubes and the growth mechanisms from the perspective of crystal growth theory is still rare, and a further understanding of the formation mechanism will be of high significance.

Theoretical and experimental studies have shown that 1D Bi-based nanomaterials could have an even larger enhancement in thermoelectric efficiency relative to their bulk and two-dimensional systems.[26,27] Bi nanowires,[13,28–30] Bi nanotubes,[6] BiSb alloy nanowires,[20,31] Bi−Sb nanowires junction,[32] and BiSb superlattice nanowires[33] arrays have been synthesized successfully in recent years by electrodeposition. Moreover, it has been shown recently that when Bi_2Te_3 nanotubes are introduced into the bulk materials the thermoelectric efficiencies will be enhanced by about 20%,[34] suggesting that Bi-based nanotubes are the promising candidates for improving the thermoelectric performances.

In this paper, we report the growth of BiSb alloy nanotubes and an abnormal growth that from polycrystalline nanotubes to single crystalline nanowires through polycrystalline nanowires was found. A possible growth mechanism from the perspective of crystal growth theory was discussed.

Experimental Methods

The AAM was prepared used the same procedure as reported in our previous paper.[20] The pore size of the AAM used is about 70 nm. The electrolyte for the deposition of $Bi_{0.5}Sb_{0.5}$ alloy nanotube contains a mixture of 0.04 M/L $BiCl_3$, 0.08 M/L $SbCl_3$, 40 g/L tartaric acid, 50 g/L citric acid, 100 g/L glycerol, 70 g/L NaCl, and 1.0 M/L HCl. The pH value of the electrolyte was adjusted to 0.82 by adding appropriate amounts of 5 mol/L aqueous ammonia. The deposition temperature is maintained at 36 °C with a water bath. $Bi_{0.5}Sb_{0.5}$ alloy was obtained at a pulsed potential of −2.0 V with a pulsed time of 8 ms and a delayed time of 12 ms.

Power X-ray diffraction (XRD, Philips PW 1700x with Cu Kα radiation), field-emission scanning electron microscopy (FE-SEM; FEI Sirion-200), transmission electron microscopy (TEM and HRTEM, JEOL-2010), and selected area electron diffraction (SAED) were used to study crystalline structure and morphology of the nanotubes array. The chemical composition was determined by energy dispersive spectrometry (EDS). For XRD measurements, the overfilled nanowires on the surface of the AAM were mechanically polished away. For SEM observations, the AAM was partly dissolved with 0.5 M NaOH solution and

* To whom correspondence should be addressed. Fax: +86-551-5591434. E-mail address: ghli@issp.ac.cn.

10.1021/jp8004986 CCC: $40.75
Published on Web 05/03/2008

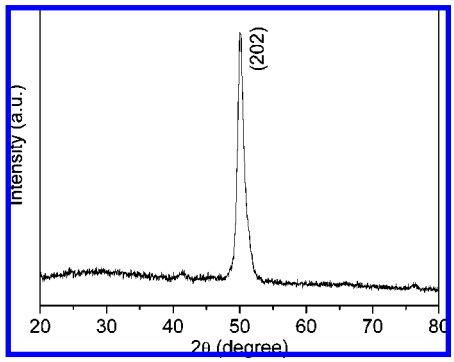

Figure 1. XRD pattern of the BiSb alloy array.

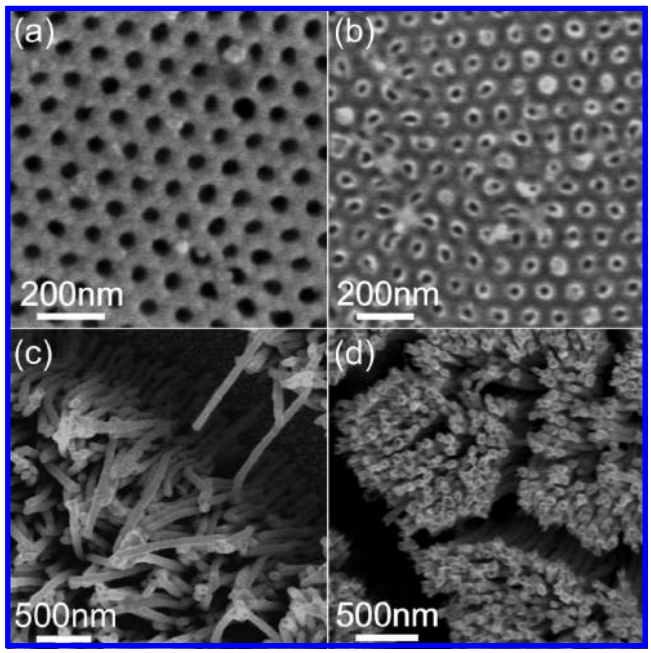

Figure 2. SEM images of (a) backside of the AAM with partially covered Au electrode−film, (b) topside of the Au electrode after AAM totally dissolved, and (c) topside and (d) bottomside view of the BiSb alloy nanotube−nanowire arrays after AAM completely dissolved.

then carefully rinsed with deionized water several times. For TEM observations, the AAM was completely dissolved with 1 M NaOH solution and then rinsed with absolute ethanol.

Results and Discussion

Figure 1 shows an XRD pattern of an as-prepared sample. The diffraction peak can be indexed to the Rhombohedral space group $\bar{R}3m$ (to which Bi, Sb, and Bi−Sb alloys belong), and a very strong diffraction peak at 49.96° indicates a preferential orientation growth along [202] direction. The 2θ value of the diffraction peak is between the positions expected for a pure Bi and Sb, indicating the formation of a Bi−Sb solid solution (the atomic ratio of Bi to Sb is about 1:1, as determined by EDS; see Figure S1 and Table S1).

Figure 2 shows SEM images of the AAM with partially covered Au electrode−film and the BiSb alloy array in which the AAM pores still can be clearly seen; see Figure 2a (the backside view) and Figure 2b (the topside view). The topside view (Figure 2c) clearly demonstrates that the top ends of the alloy array are nanowires, while the bottomside view (Figure 2d) displays the formation of nanotubes at the bottom of the

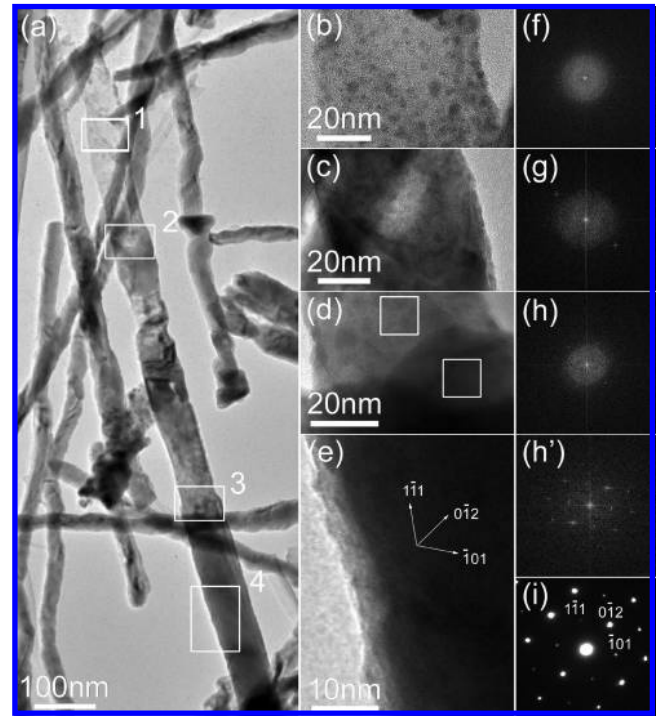

Figure 3. (a) TEM image of a nanotube−nanowire junction. (b−e) HRTEM images of the area marked with the rectangles 1−4 shown in panel a. (f,g) 2D FFT of panels b and c. (h,h′) The FFT of the area marked with the rectangles 1 and 2 shown in panel d; (i) the SAED pattern of panel e.

array. This result indicates that the as-prepared BiSb alloy array is a nanotube−nanowire junction array. From Figure 2, one also can see that the average diameter of the nanowires is about 70 nm, which is consistent with the AAM pore size.

Figure 3 shows the TEM image of a nanotube−nanowire junction. The junction contains a polycrystalline nanotube−nanowire segment with a length of about 820 nm (the nanotube is about 360 nm) and a single crystalline nanowire segment with a diameter of about 70 nm; see Figure 3a. The HRTEM image of the nanotube section (Figure 3b), corresponding to the first rectangle in Figure 3a, shows some small grains on the wall, implying a polycrystalline structure. No diffraction rings or points can be found for the corresponding fast Fourier transforms (FFT, Figure 3f) due to the poor lattice fringes in the HRTEM image and a very thin nanotube wall (about 10 nm). The HRTEM image of the junction area of the polycrystalline nanotube−nanowire (Figure 3c), the second rectangle in Figure 3a, still shows some small grains, and the corresponding FFT (Figure 3g) displays two diffraction points and does not change significantly in the whole area of the HRTEM image. The HRTEM image of the nanowire area (Figure 3d, the third rectangle in Figure 3a), clearly shows the transition of the nanowire from polycrystalline to single crystalline structure, the boundary that spans the bottom-side with a lattice fringe and the top-side with a vague lattice fringe also can be clearly seen. The FFT (shown in Figure 3h and Figure 3h′), corresponding to the first and second white rectangle in Figure 3d, further confirmed the transition of the nanowire from polycrystalline to single crystalline structure. The HRTEM image of the single crystalline nanowire section (Figure 3e, the fourth rectangle in Figure 3a) shows a clear lattice fringe, and the corresponding diffraction points (Figure 3i) are sharp and bright, indicating the single crystalline structure.

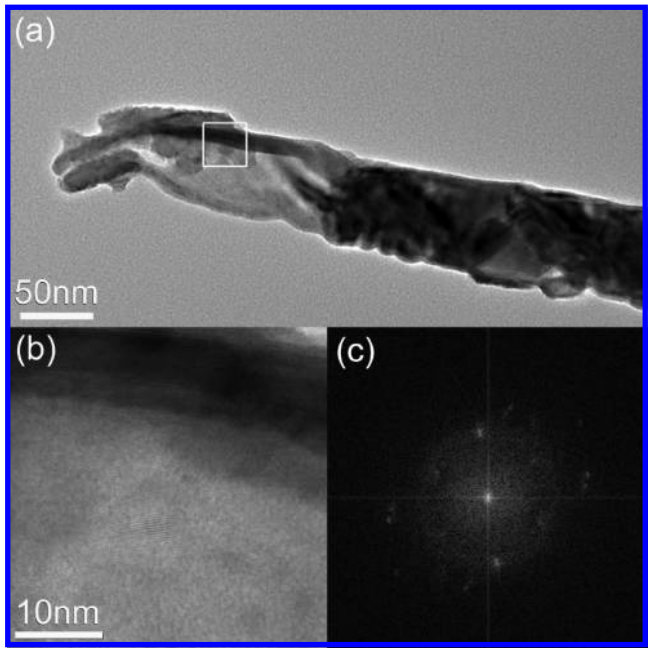

Figure 4. (a) TEM image of a polycrystalline nanotube−nanowire junction. (b) HRTEM image of the area marked with the rectangle shown in panel a. (c) FFT of panel b.

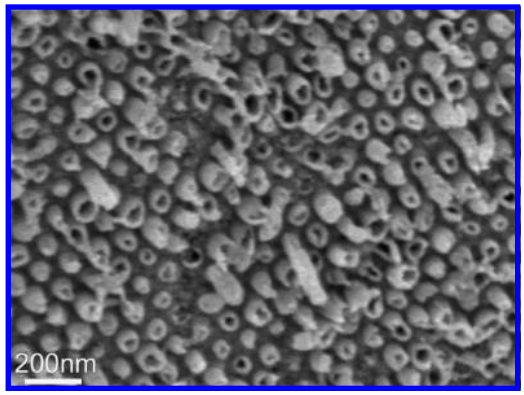

Figure 5. SEM image of a nanotubes array with AAM totally dissolved.

Further TEM observations were performed to study the structure of the nanotube, as shown in Figure 4. The nanotube has a length of about 200 nm, a diameter of about 62 nm, and a wall thickness of about 10 nm. From the HRTEM image (Figure 4b) of the area marked with a rectangle in Figure 4a, one can clearly see the different grains with separate lattice fringes, and the corresponding FFT (Figure 4c) further proved the polycrystalline structure.

To study the initial growth of the nanotubes, a very short deposition time was performed, and the obtained array only has an average length of about 300 nm. SEM topside view (Figure 5) clearly demonstrates that the initial grown array is nanotube. Figure 6 shows the TEM image of the nanotubes in which the corresponding SAED pattern (shown in the bottom inset) clearly shows a ring shape, proving that the nanotubes have a polycrystalline structure. The lattice fringes in different areas corresponding to different grains also can be clearly seen in the HRTEM image (the top inset, two grains have different [012] orientations), which further proved the polycrystalline structure of the nanotubes.

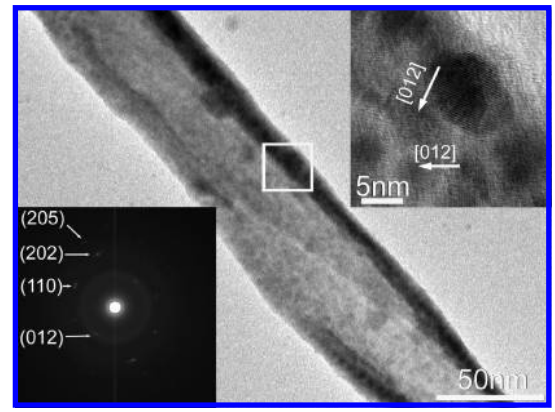

Figure 6. TEM image of a polycrystalline nanotube. The top inset is the HRTEM image of the area marked with a rectangle and the bottom inset is the corresponding SAED pattern.

As pointed by Tian et al.[18] the single crystalline nanowire growth via a 2D layer-by-layer epitaxial mechanism is relatively facile for low melting point metals such as Bi at room temperature, and our previous results had proved that elemental Bi,[13,28–30] Sb,[11] and BiSb alloy[20,31] single crystalline nanowires could be grown by the pulsed electrodeposition. The growth mechanism of the electrodeposited single crystalline nanowires that has been generally considered follows a 3D to 2D transition mode.[18–20] It has been proven that single element nanotubes could be obtained by electrodeposition.[6–9,15–17,25] Polycrystalline alloy nanotubes with a large diameter have also been fabricated,[10,21,23] but the origin of the initial formation of nanotubes is still not clear. If single crystalline nanotubes could be synthesized, whether the growth of polycrystalline nanotubes could maintain remains an open question.

In the present study, the BiSb alloys are deposited on an amorphous Au film that did not fully cover the backside pores of the AAM. The Au film is inert with respect to the growth of the nanowires and has no effect on the nanowire growth.[35] In the initial growth stage, the BiSb nuclei is random, and a newly coalesced compact deposit has perfectly random orientation;[19] therefore, a 3D growth mode will result in the formation of polycrystalline BiSb nanotubes in the initial growth stage. Fukunaka et al.[24] studied the initial growth of the electrodeposited Ni nanowires in nanoporous templates and pointed out that a transition from nanotube to nanowire at the growth front resulted because the growth rate along the length is about 10 times faster than that of the tube wall. They also deduced that the growth of metallic nanotubes is not feasible by electrodeposition if the growing grains readily become comparable to the pore size of the employed AAM. Ni is an inert metal with a high melting point, and the surface diffusion coefficient of the adatoms is low and thus tends to form a new nucleus. In fact, when there is growth with a direct current deposition, the nucleation rate in the growing front will increase due to the ion concentration gradient along the axis of the pores of the template, which will lead to a thicker and thicker nanotube consisted of fine Ni grains, and finally result in a vaulted close of the nanotube. Figure 7a schematically illustrates the gradual transition from nanotube to nanowire in which the growth rate along the length V_1 is larger than that along the tube wall V_2, and the whole length of the as-deposited nanotube L equals to L_t, which is the transition length from nanotube to nanowire. In the present study the transition from the BiSb polycrystalline nanotube to polycrystalline nanowire is an abrupt one rather than a gradual one, as shown in Figure 7b. In our case, the L

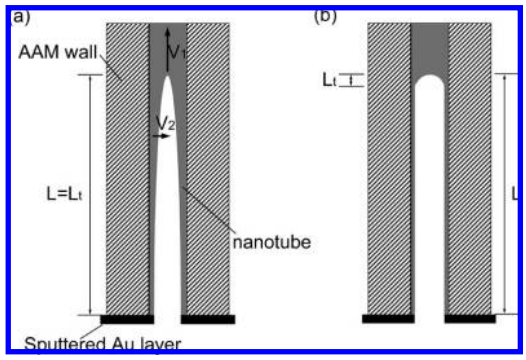

Figure 7. Schematic illustration of the transition from nanotube to nanowire with (a) a gradual process and (b) an abrupt process.

value is much larger than L_t, and L_t has the same or smaller value as the pore diameter R. One also could see that $V_1 \gg V_2$ before the transition; if $V_1 \leq V_2$, then $L \leq R$ and this obviously conflicts with our results. However, in the transition region, because $L_t \leq R$, then $V_1 \leq V_2$. Therefore, it is speculated that there is an abnormal grain growth that results in the abrupt close of the nanotube. Bi is a low melting point metal, and the surface diffusion coefficient is high for the adatoms, which will lead to an increased grain size. With the increase of the average grain size, an abnormal grain growth could happen.

In the abnormal grain growth, the growth of a subpopulation of grains is favored, and a nonself-similar distribution will at least temporarily develop until all grains that are not in the subpopulation are eliminated.[36] The competitive growth of different grains with different size that will result in a small population of grains continues to grow whereas the majority fine grains either do not grow at all or grow very slow, leading to the transition from the polycrystalline nanotube to a polycrystalline nanowire. This phenomenon might be verified by the change of the SAED pattern from ring to point due to the decreased number of grains. After the transition, the growth of the polycrystalline nanowire follows a common 3D to 2D transition mode and finally results in the formation of single crystalline nanowire. Nevertheless, our result does not exclude the transition from a polycrystalline nanotube to a single crystalline nanotube.

Polycrystalline nanotube structure could be maintained only if the growth rate along the nanotube axis is much higher than that normal to the nanotube. This could be happened for those metals with high melting points and at a high deposition rate. Appropriate surfactant additives might be helpful to the growth of nanotubes along the membrane walls. In the pulsed electrodeposition of BiSb alloys, the growth rate will decrease with an abrupt decrease of the cathodic current after the initial deposition. The reduced ions will have more time to relax to a more stable state and thus will subsequently lead to the abnormal grain growth and result in the close of nanotube. This kind of abrupt transition from polycrystalline nanotube to polycrystalline nanowire is considered to happen in the electrodeposition process of low melting points metals, such as BiSb in the present study.

Conclusions

In summary, BiSb alloy nanotube−nanowire array has been fabricated by the pulsed electrodeposition technique. The growth of the polycrystalline nanotubes is terminated by polycrystalline nanowires abruptly and then follows by single crystalline nanowires. The initial formation mechanism of the nanotubes follows a 3D growth mode, and the transition from the polycrystalline nanotube to polycrystalline nanowire takes place abruptly due to an abnormal grain growth. The change from polycrystalline nanowire to single crystalline nanowire follows the common 3D to 2D transition process. The understanding about the growth mechanism of the electrodeposited nanotubes is of great importance in the controlling synthesis of nanotubes, and we speculate that the BiSb polycrystalline nanotube-polycrystalline nanowire-single crystalline nanowire junction structure might have potential applications in thermoelectric field.

Acknowledgment. This work was supported by the National Natural Science Foundation of China (No. 10704074).

Supporting Information Available: EDS characteraction of the BiSb alloy. This information is available free of charge via the Internet at http://pubs.acs.org.

References and Notes

(1) Zhao, Y. M.; Hu, W. B.; Xia, Y. D.; Smith, E. F.; Zhu, Y. Q.; Dunnill, C. W.; Gregory, D. H. *J. Mater. Chem.* **2007**, *17*, 4436.
(2) Fang, X. S.; Bando, Y.; Ye, C. H.; Golberg, D. *Chem. Commun.* **2007**, *29*, 3048.
(3) Fang, X. S.; Bando, Y.; Ye, C. H.; Shen, G. Z.; Gautam, U. K.; Tang, C. C.; Golberg, D. *Chem. Commun.* **2007**, *40*, 4093.
(4) Xia, Y.; Yang, P.; Sun, Y.; Wu, Y.; Mayers, B.; Gates, B.; Yin, Y.; Kim, F.; Yan, H. *Adv. Mater.* **2003**, *15*, 353.
(5) Sander, M. S.; Gao, H. *J. Am. Chem. Soc.* **2005**, *127*, 12158.
(6) Li, L.; Yang, Y. W.; Huang, X. H.; Li, G. H.; Ang, R.; Zhang, L. D. *Appl. Phys. Lett.* **2006**, *88*, 103119.
(7) Li, L.; Xiao, Y.; Yang, Y.; Huang, X.; Li, G.; Zhang, L. *Chem. Lett.* **2005**, *34*, 930.
(8) Fukunaka, Y.; Motoyama, M.; Konishi, Y.; Ishii, R. *Electrochem. Solid-State Lett.* **2006**, *9*, C62.
(9) Lee, W.; Alexe, M.; Nielsch, K.; Gosele, U. *Chem. Mater.* **2005**, *17*, 3325.
(10) Davis, D. Electrodeposition of Multilayered Nanostructures for Giant Magnetoresistance and Thermoelectric Applications. Ph.D. Thesis, Louisiana State University, May, 2007.
(11) Zhang, Y.; Li, G.; Wu, Y.; Zhang, B.; Song, W.; Zhang, L. *Adv. Mater.* **2002**, *14*, 1227.
(12) Nielsch, K.; Müller, F.; Li, A.-P.; Gösele, U. *Adv. Mater.* **2000**, *12*, 582.
(13) Li, L.; Zhang, Y.; Li, G.; Zhang, L. *Chem. Phys. Lett.* **2003**, *378*, 244.
(14) Liu, J.; Duan, J. L.; Toimil-; Molares, M. E.; Karim, S.; Cornelius, T. W.; Dobrev, D.; Yao, H. J.; Sun, Y. M.; Hou, M. D.; Mo, D.; Wang, Z. G.; Neumann, R. *Nanotechnology* **2006**, *17*, 1922.
(15) Zhang, X. Y.; Wang, H. T.; Bourgeois, L.; Pan, R. J.; Zhao, D. Y.; Webley, P. A. *J. Mater. Chem.* **2008**, *18*, 463.
(16) Brumlik, C. J.; Martin, C. R. *J. Am. Chem. Soc.* **1991**, *113*, 3174.
(17) Bao, J.; Tie, C.; Xu, Z.; Zhu, Q.; Shen, D.; Ma, Q. *Adv. Mater.* **2001**, *13*, 1631.
(18) Tian, M.; Wang, J.; Kurtz, J.; Mallouk, T. E.; Chan, M. H. W. *Nano Lett.* **2003**, *3*, 919.
(19) Pan, H.; Liu, B.; Yi, J.; Poh, C.; Lim, S.; Ding, J.; Feng, Y.; Huan, C. H. A.; Lin, J. *J. Phys. Chem. B* **2005**, *109*, 3094.
(20) Dou, X. C.; Zhu, Y. G.; Huang, X. H.; Li, L.; Li, G. H. *J. Phys. Chem. B* **2006**, *110*, 21572.
(21) Davis, D. M.; Podlaha, E. J. *Electrochem. Solid-State Lett.* **2005**, *8*, D1.
(22) Davis, D.; Moldovan, M.; Young, D.; Podlaha, E. *ECS Meeting Abstracts* **2006**, *502*, 621.
(23) Davis, D. M.; Moldovan, M.; Young, D. P.; Henk, M.; Xie, X.; Podlaha, E. J. *Electrochem. Solid-State Lett.* **2006**, *9*, C153.
(24) Motoyama, M.; Fukunaka, Y.; Sakka, T.; Ogata, Y. H. *Electrochim. Acta* **2007**, *53*, 205.
(25) Yoo, W.-C.; Lee, J. K. *Adv. Mater.* **2004**, *16*, 1097.
(26) Heremans, J.; Thrush, C. M.; Zhang, Z.; Sun, X.; Dresselhaus, M. S.; Ying, J. Y.; Morelli, D. T. *Phys. Rev. B* **1998**, *58*, R10091.
(27) Lin, Y. M.; Sun, X. Z.; Dresselhaus, M. S. *Phys. Rev. B* **2000**, *62*, 4610.
(28) Li, L.; Yang, Y.; Fang, X.; Kong, M.; Li, G.; Zhang, L. *Solid State Commun.* **2007**, *141*, 492.
(29) Li, L.; Zhang, Y.; Yang, Y. W.; Huang, X. H.; Li, G. H.; Zhang, L. D. *Appl. Phys. Lett.* **2005**, *87*, 031912.

(30) Li, L.; Zhang, Y.; Li, G.; Wang, X.; Zhang, L. *Mater. Lett.* **2005**, *59*, 1223.
(31) Li, L.; Li, G.; Zhang, Y.; Yang, Y.; Zhang, L. *J. Phys. Chem. B* **2004**, *108*, 19380.
(32) Zhang, Y.; Li, L.; Li, G. H. *Nanotechnology* **2005**, *16*, 2096.
(33) Xue, F. H.; Fei, G. T.; Wu, B.; Cui, P.; Zhang, L. D. *J. Am. Chem. Soc.* **2005**, *127*, 15348.
(34) Zhao, X. B.; Ji, X. H.; Zhang, Y. H.; Zhu, T. J.; Tu, J. P.; Zhang, X. B. *Appl. Phys. Lett.* **2005**, *86*, 062111.
(35) Amblart, J. F., M.; Maurin, G.; Spyrellis, N.; Trevisan-Souteyrand, E. T. *Electrochim. Acta* **1983**, *28*, 909.
(36) Thompson, C. V. *Annu. Rev. Mater. Sci.* **1990**, *20*, 245.

JP8004986